Normal state charge dynamics of $Fe_{1.06}Te_{0.88}S_{0.14}$ superconductor probed with infrared spectroscopy

N. Stojilovic,[1] A. Koncz,[2] L. W. Kohlman,[2] Rongwei Hu,[3,*] C. Petrovic,[3] and S. V. Dordevic[2,†]
[1]*Department of Physics and Astronomy, University of Wisconsin Oshkosh, Oshkosh, Wisconsin 54901, USA*
[2]*Department of Physics, The University of Akron, Akron, Ohio 44325, USA*
[3]*Condensed Matter Physics and Materials Science Department, Brookhaven National Laboratory, Upton, New York 11973, USA*
(Received 9 February 2010; revised manuscript received 27 April 2010; published 19 May 2010)

We have used optical spectroscopy to probe the normal state electrodynamic response of $Fe_{1.06}Te_{0.88}S_{0.14}$, a member of the 11 family of iron-based superconductors with $T_c = 8$ K. Measurements have been conducted over a wide frequency range (50–50 000 cm^{-1}) at selected temperatures between 10 and 300 K. At low temperatures the material behaves as an "incoherent metal:" a Drude-type peak is absent from the optical conductivity and all optical functions reveal that quasiparticles are not well defined down to the lowest measured temperature. We introduce "generalized spectral weight" analysis and use it to track temperature induced redistribution of spectral weight. Our results, combined with previous reports, indicate that the 11 family of iron-based superconductors might be different from other families.

DOI: 10.1103/PhysRevB.81.174518 PACS number(s): 74.25.nd, 78.15.+e, 78.30.−j

I. INTRODUCTION

Iron-based superconductors are currently at the focus of condensed-matter research. Discovered 2 years ago,[1] these materials have attracted attention not only because of their high critical temperatures but also because of their similarities with cuprates. Their phase diagram resembles that of the cuprates, most notably, the superconducting state seems to develop from an unconventional normal state, after magnetic order is destroyed by doping. They are also layered materials, consisting of FeAs, FeTe, FeS, or FeSe planes, separated by spacer layers. However, there are also some important differences. Most notably, the parent compounds of cuprates are antiferromagnetic insulators, whereas the parent compounds of iron-based superconductors are antiferromagnetic spin-density-wave (SDW) metals.[2]

Optical spectroscopy is a powerful probe of electrodynamic response of high-T_c superconductors.[3–5] Optical constants provide insight into low-energy excitations and charge dynamics, critical for understanding physics of strongly correlated systems. The information obtained from optical constants can be used to test existing theories and/or stimulate development of new theoretical models. Optical spectroscopy is also a crucial experimental method for electronic band-structure determination.

Several families of iron-based superconductors have been discovered and they are conveniently refereed to as the "11," "1111," or "122" families.[5] The 11 family is peculiar because the spacer layers are absent, and it is believed that this family will allow the intrinsic properties of iron-containing planes to be isolated. However, most of optical studies so far have focused on the 122 family[6–13] (and to a lesser extent 1111 family[14,15]) for which large single crystals can be grown. In this work, we have investigated the electrodynamic response of a member of the 11 (FeTe) family. The only previous infrared (IR) study on 11 family was on a nonsuperconducting $Fe_{1.05}Te$ (Ref. 16).

Structural analysis has shown that the exact chemical composition of the analyzed sample is $Fe_{1.06}Te_{0.88}S_{0.14}$ (Ref. 17). Note that in addition to being doped with S, this sample also has 6% of excess iron, which might play important role in charge dynamics.[16,18] Magnetization measurements have revealed that the studied system undergoes structural and magnetic transitions, with transition temperature around 23 K (Ref. 17). Transport measurements on the other hand do not display any signatures of these transitions, and dc resistivity monotonically increases as temperature decreases down to 8 K, when the system undergoes superconducting transition and the resistivity abruptly drops to zero.

IR reflectance measurements were performed at The University of Akron on a Bruker IFS 66v/s, whereas UV-visible experiments were conducted using Varian/Cary 300. An overfilling technique was used to obtain the absolute values of reflectance from the sample with surface area of approximately 1 mm × 1 mm (Ref. 19). Electrodynamic response was probed in the frequency range 50–50 000 cm^{-1} (6 meV–6.2 eV) and as a function of temperature in the range 10–300 K, all in the normal state. The optical constants were extracted from reflectance data using Kramers-Kronig (KK) analysis. In addition, we have performed magneto-optical measurements at 4.2 K (in the superconducting state) with magnetic fields up to 18 T.

II. EXPERIMENTAL RESULTS

Figure 1 displays raw reflectance data $R(\omega)$ and the real part of optical conductivity $\sigma_1(\omega)$. The absolute value of reflectance gradually decreases with frequency from about 0.9 at 50 cm^{-1} to about 0.25 at 50 000 cm^{-1}, which can be interpreted as metallic behavior. However the temperature dependence is opposite from expected,[20] as the reflectivity decreases with decreasing temperature. This anomalous behavior is even more obvious in $\sigma_1(\omega)$: zero-energy (Drude-type) peak is absent from the data (except maybe at 300 K) and the conductivity decreases monotonically with decreasing temperature at the lowest measured frequencies. This result indicates that at low temperatures quasiparticles are not well defined, which will become even more obvious from the

 ©2010 The American Physical Society

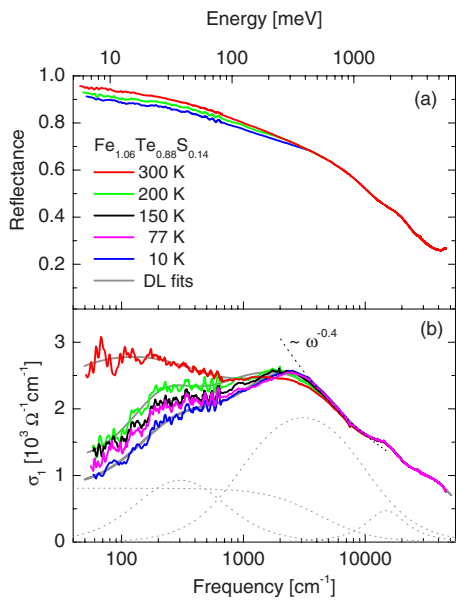

FIG. 1. (Color online) (a) Raw reflectance data of iron-based superconductor $Fe_{1.06}Te_{0.88}S_{0.14}$ at several different temperatures ranging from 10 K to room temperature. The temperature dependence is restricted to the region below about 4000 cm^{-1}. (b) The optical conductivity $\sigma_1(\omega)$ extracted directly from reflectance using KK analysis. The total DL fit as well as the individual components of the fit are shown with gray lines. The dashed black line is the fit to the power-law behavior at higher frequencies.

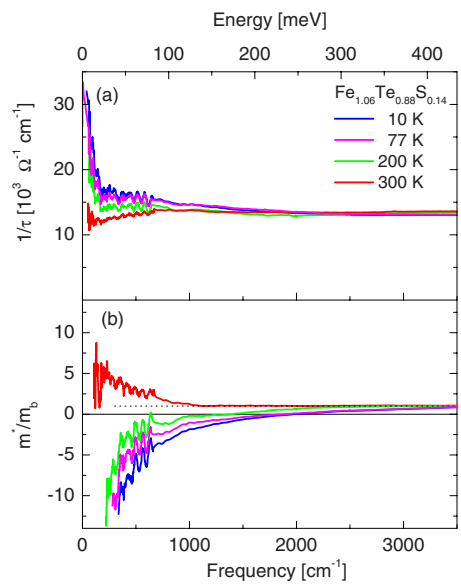

FIG. 2. (Color online) Optical scattering rate $1/\tau(\omega)$ and effective mass $m^*(\omega)/m_b$ obtained from Eqs. (1) and (2). Both optical functions reveal the failure of the quasiparticle concept at low temperatures.

extended Drude analysis below. $Fe_{1.06}Te_{0.88}S_{0.14}$ therefore can be considered to be an "incoherent metal."[21]

Although the overall behavior of reflectance is metallic, the plasma edge cannot be clearly resolved in the spectra, as reflectance gradually decreases with frequency. At higher frequencies the response is dominated by interband transitions but they also are not easily discerned in the spectra. A shoulder in optical conductivity around 14 000 cm^{-1} (1.7 eV) may originate from transitions involving iron 3*d* states, similar to what was predicted by Haule *et al.*[22] in a theoretical study of another iron-based superconductor. We also do not observe any phonon peaks in the far IR, similar to $Fe_{1.05}Te$ (Ref. 16). Structural and magnetic transitions at 23 K do not seem to have any significant effect on optical spectra.

Theoretical calculations of FeSe, based on local-density approximation with dynamical meana field theory (LDA +DMFT), predicted incoherent metal with a pseudogap at low frequencies,[21] in accord with our results. These calculations also predict a smooth crossover of optical conductivity to a power-law behavior $\simeq\omega^{-\eta}$ at higher frequencies.[21] Dashed black line in Fig. 1(b) represents the best fit to the optical conductivity and the obtained power law $\eta\simeq 0.4$.

To gain further insight into the electronic properties of $Fe_{1.06}Te_{0.88}S_{0.14}$ we fit the data using a standard Drude-Lorentz (DL) model.[3,4,20] The minimal model to achieve a good fit consisted of a Drude and three Lorentzian modes, centered at around 300, 3000, and 14 800 cm^{-1}. At room temperature the best fit to the data yields for the plasma frequency of the Drude component $\omega_{p,D}=35\,600$ cm^{-1} (4.4 eV) but this value should be taken cautiously. The total fits at all temperatures, as well as the three individual contributions at 10 K, are shown in Fig. 1(b) with gray lines. The lowest lying oscillator displays most prominent temperature dependence. Its energy and intensity grow significantly as temperature decreases. The mid-IR peak at 3000 cm^{-1} (372 meV) might be a generic feature of iron-based superconductors; similar peaks have been observed in other families.[5] The oscillator at 14 800 cm^{-1} simulates the effect of interband transitions, presumably involving iron 3*d* states, as discussed above.

In the one-component approach one assumes that only a single type of carriers are present in the system but their scattering rate acquires frequency dependence.[3,4,20] Within the so-called "extended" Drude model one calculates the optical scattering rate $1/\tau(\omega)$ and effective mass $m^*(\omega)/m_b$ from the complex optical conductivity $\sigma(\omega)$ as

$$\frac{1}{\tau(\omega)} = \frac{\omega_p^2}{4\pi}\Re\left[\frac{1}{\sigma(\omega)}\right], \tag{1}$$

$$\frac{m^*(\omega)}{m_b} = \frac{\omega_p^2}{4\pi}\Im\left[\frac{1}{\sigma(\omega)}\right]\frac{1}{\omega}, \tag{2}$$

where the plasma frequency $\omega_p^2=4\pi e^2 n/m_b$ (n is the carrier density and m_b their band mass) can be estimated from the integration of $\sigma_1(\omega)$ up to the frequency of the onset of interband absorption. However, as pointed out above, the plasma edge is not very prominent in the spectra of $Fe_{1.06}Te_{0.88}S_{0.14}$, rendering the value of plasma frequency ambiguous. Instead, we fit the value of ω_p in Eq. (2) so that the effective mass at frequencies around 3500 cm^{-1} is equal to unity [dashed line in Fig. 2(b)]. The best fit is achieved for $\omega_p=26\,000$ cm^{-1} (3.2 eV), a value which is almost 30% smaller than the plasma frequency of the Drude component extracted above. The results of the analysis are shown in Fig.

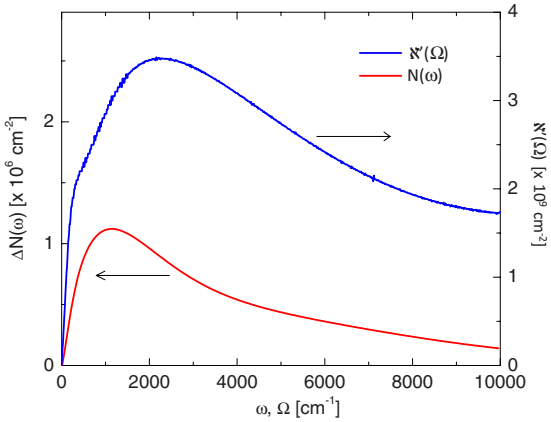

FIG. 3. (Color online) Spectral weight [Eq. (5)] and generalized spectral weight [Eq. (6)] analysis for $Fe_{1.06}Te_{0.88}S_{0.14}$ at $T_1=10$ K and $T_2=77$ K.

2 and the features of an incoherent metal are now obvious. The scattering rate is relatively flat and featureless at room temperature but at low temperatures it develops a peak below 180 cm^{-1}. The effective mass, on the other hand, becomes negative. These features of the spectra are indications that the quasiparticle concept, on which the extended Drude model is based, is not applicable at low temperatures.

III. GENERALIZED SPECTRAL WEIGHT ANALYSIS

Model-independent sum rules are important tools in condensed-matter physics.[23] The so-called effective spectral weight function $N(\omega)$ is frequently used for the analysis of IR spectra. It is defined as[3,20]

$$N(\omega) = \int_0^{\omega} \sigma_1(x)dx \tag{3}$$

and for $\omega \to \infty$ it becomes the global oscillator strength sum rule,

$$N(\infty) = \int_0^{\infty} \sigma_1(x)dx = \frac{\pi n e^2}{2m_e}, \tag{4}$$

which is a statement on the conservation of electric charge.[23] Equation (3) is often used to quantify spectral weight redistribution between temperatures T_1 and T_2 in the form

$$\Delta N(\omega) = N_{T_1}(\omega) - N_{T_2}(\omega). \tag{5}$$

Figure 3 shows the results of this analysis applied to $Fe_{1.06}Te_{0.88}S_{0.14}$ at $T_1=77$ K and $T_2=10$ K. $\Delta N(\omega)$ has a characteristic shape, which indicates that the spectral weight is removed from the low-frequency region, below 1000 cm^{-1} and is transferred to higher frequencies, in the region around 2000–4000 cm^{-1}. Within the error bars, the spectral weigh is recovered by the mid-IR region. However, $\Delta N(\omega)$ spectrum cannot reveal the energy scale at which the transfer of spectral weight occurs.

In order to address this question we introduce "generalized spectral weight" function $\aleph(\Omega)$,

$$\aleph(\Omega) = \int_0^{\infty} \sigma_1^{T_1}(x+\Omega)\sigma_1^{T_2}(x)dx. \tag{6}$$

The idea comes from the correlation functions frequently used in signal processing.[24] In signal processing, cross correlation is a measure of similarity of two wave forms as a function of a lag applied to one of them. Correlation functions are a useful indicator of dependencies as a function of distance in time, space, or energy (or frequency in case of infrared spectra) and are used to assess the distance required between sample points for the values to be maximally correlated or to be effectively uncorrelated. Recently (auto)correlation function was used for the analysis of angle resolved photoemission spectroscopy (ARPES) data, where it is directly related to the quasiparticle density of states.[25] Note that $\aleph(\Omega)$ in Eq. (6) is a function of the frequency lag Ω, not the upper integration limit ω. Function $\aleph(\Omega)$ is expected to display characteristic features at the values of frequency shifts Ω that connect regions between which a large amount of spectral weight is transferred (i.e., regions which are maximally correlated). In practical applications, function $\aleph(\Omega)$ is usually dominated by the spectral weight which does not participate in redistribution and these characteristic features might not be obvious. In those cases the first derivative of $\aleph(\Omega)$ is useful. Examples of these calculations, as well as the very important question of conservation of generalized spectral weight function, will be presented in a separate publication.[26]

In Fig. 3 we show the results of generalized spectral weight analysis [Eq. (6)] applied to $Fe_{1.06}Te_{0.88}S_{0.14}$ at $T_1=77$ K and $T_2=10$ K. The $\aleph(\Omega)$ is dominated by the spectral weight that does not participate in transfer, so instead we display the first derivative $\aleph'(\Omega)$. The $\aleph'(\Omega)$ spectrum reveals a broad peak centered around 2250 cm^{-1} (280 meV). We take this as the characteristic energy scale over which the majority of spectral weight is transferred between 10 and 77 K.

IV. DISCUSSION

In a density-functional study of FeS, FeSe, and FeTe it was reported that the Fermi surface and electronic structure of these compounds is similar to those of iron pnictides (1111 and 122 families).[27] Therefore, the 11 family was supposed to be a model system in which to study the intrinsic properties of iron-containing planes. However, our results, combined with previous IR studies, indicate that there might be some important differences between the electronic structure of 11 and the other families.

The reflectance of $Fe_{1.06}Te_{0.88}S_{0.14}$ is similar to the reflectance of $Fe_{1.05}Te$ (Ref. 16). In the far-IR region the reflectance of $Fe_{1.05}Te$ decreases with decreasing temperature, resulting in a reduction in conductivity in far-IR region, similar to what we observe in $Fe_{1.06}Te_{0.88}S_{0.14}$. Chen *et al.*[16] speculate that this incoherent transport in $Fe_{1.05}Te$ is caused by strong scattering from excess iron. However, there are also some important differences between $Fe_{1.06}Te_{0.88}S_{0.14}$ and $Fe_{1.05}Te$. We observe no rapid increase in conductivity at low frequencies for 10 K measurements. On the other hand in

$Fe_{1.05}Te$ a narrow Drude-type peak develops in the optical conductivity at low temperatures. This coherent behavior appears below structural and magnetic phase transition at 65 K, which implies that it is related to SDW order. In $Fe_{1.05}Te$ this phase transition has stronger influence on charge transport than in $Fe_{1.06}Te_{0.88}S_{0.14}$: the dc resistivity changes character from insulating to metallic below the transition.

Incoherent charge transport in the 11 family should be contrasted with a coherent response which has been observed in 1111 (Refs. 14 and 15) and 122 families.[6–12] Infrared spectra of both undoped (parent) and doped phases of these families display well-defined Drude-type modes. Similar to $Fe_{1.05}Te$ SDW transition has a dramatic effect on their optical properties. The response of parent compounds $BaFe_2As_2$ and $SrFe_2As_2$ becomes even more coherent below the SDW transitions[7] as the width of Drude mode is reduced by an order of magnitude. The infrared spectra of these parent compounds are dominated by the mid-IR peak, which may have the same origin as the peak we observe in $Fe_{1.06}Te_{0.88}S_{0.14}$ around 3000 cm^{-1} (372 meV).

The absence of SDW gap from IR spectra of both $Fe_{1.06}Te_{0.88}S_{0.14}$ and $Fe_{1.05}Te$ (Ref. 16) is also interesting. Recent ARPES study of a parent compound $Fe_{1+x}Te$ (Ref. 28) has also revealed that the SDW gap is absent. Optical spectra reveal that spectral weight is shifting with temperature and the generalized spectral weight analysis we introduced indicates that a typical energy scale for the shift is about 280 meV. The spectral weight of $Fe_{1.06}Te_{0.88}S_{0.14}$ is removed from the low-energy region, which can be interpreted as a pseudogap feature, however we point out that this behavior starts already at room temperature (Fig. 1) and therefore is unlikely to be related to SDW transition. All this indicates that the electronic structure of the 11 family might be different from the 1111 and 122 families, for which clear signatures of SDW gaps have been observed.[5] IR studies on these two families have found a gap (or even several gaps) in the excitation spectra. On the other hand both the parent compound[16] and a doped sample studied in this work did not reveal the presence of a gap in their excitation spectra.

Finally, we address what happens below 8 K, when the system becomes superconducting. We have performed magneto-optical studies at 4.2 K in 18 T superconducting magnet at the National High Magnetic Field Laboratory. Figure 4 displays the results of these measurements. The magnetoreflection ratio $R(18\ \mathrm{T})/R(0\ \mathrm{T})$ is shown as a function of frequency. Apart from the vertical offset,[29] within the noise level the ratio is a straight line, which indicates the absence of field-induced effects in $Fe_{1.06}Te_{0.88}S_{0.14}$. This is in contrast with $BaFe_{2-x}Co_xAs_2$ with $T_c=22$ K (optimally doped member of the 122 family), where clear field-induced changes have been observed caused by the suppression of the superconducting gap.[30] We speculate that field-induced changes in $Fe_{1.06}Te_{0.88}S_{0.14}$ are not observed because either they are below the detection limit of our experiment or because the superconductiong gap is outside of our frequency window.

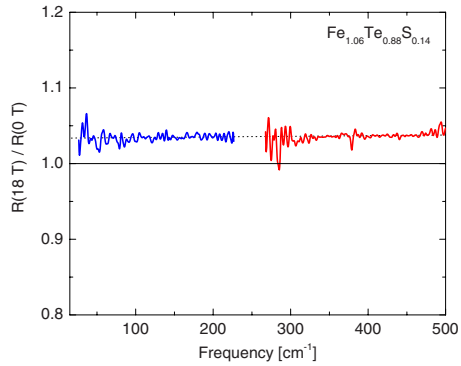

FIG. 4. (Color online) Magneto-optical ratio $R(18\ \mathrm{T})/R(0\ \mathrm{T})$ obtained at 4.2 K. We found no deviation from straight line, which indicates that magnetic field does not affect the optical properties. The measurement system causes vanishingly small signal intensity in the region around 250 cm^{-1} and this part of the spectrum is not shown (Ref. 29).

V. SUMMARY

In summary, we have presented the results of infrared and optical spectroscopy studies of novel iron-based superconductor $Fe_{1.06}Te_{0.88}S_{0.14}$. The results indicate incoherent normal state charge transport and absence of well-defined quasiparticles at all temperatures down to T_c. We have introduced "generalized spectral weight analysis" and used it to track redistribution with temperature. The analysis reveals that the characteristic energy scale for the spectral weight shifts is approximately 280 meV. Our results, combined with previous reports, indicate that there are important differences between 11 and other families of iron-based superconductors.

ACKNOWLEDGMENTS

We thank D.N. Basov and C.C. Homes for critical reading of the manuscript. Special thanks to R.D. Ramsier for the use of his equipment. This work was in part supported by the U.S. Department of Energy, Office of Science, Office of Basic Energy Sciences as part of the Energy Frontier Research Center (EFRC) Center for Emergent Superconductivity (CES).

*Present address: Ames Laboratory US DOE and Department of Physics and Astronomy, Iowa State University, Ames, IA 50011.
†dsasa@uakron.edu

[1] Y. Kamihara, T. Watanabe, M. Hirano, and H. Hosono, J. Am. Chem. Soc. **130**, 3296 (2008).
[2] M. R. Norman, Phys. **1**, 21 (2008).
[3] D. N. Basov and T. Timusk, Rev. Mod. Phys. **77**, 721 (2005).
[4] S. V. Dordevic and D. N. Basov, Ann. Phys. **15**, 545 (2006).
[5] W. Z. Hu, Q. M. Zhang, and N. L. Wang, Physica C **469**, 545 (2009).

[6] J. Yang, D. Huvonen, U. Nagel, T. Room, N. Ni, P. C. Canfield, S. L. Budko, J. P. Carbotte, and T. Timusk, Phys. Rev. Lett. **102**, 187003 (2009).
[7] W. Z. Hu, J. Dong, G. Li, Z. Li, P. Zheng, G. F. Chen, J. L. Luo, and N. L. Wang, Phys. Rev. Lett. **101**, 257005 (2008).
[8] F. Pfuner, J. G. Analytis, J.-H. Chu, I. R. Fisher, and L. Degiorgi, Eur. Phys. J. B **67**, 513 (2009).
[9] A. Akrap, J. J. Tu, L. J. Li, G. H. Cao, Z. A. Xu and C. C. Homes, Phys. Rev. B **80**, 180502(R) (2009).
[10] K. W. Kim, M. Rossle, A. Dubroka, V. K. Malik, T. Wolf, and C. Bernhard, arXiv:0912.0140 (unpublished).
[11] E. van Heumen, Y. Huang, S. de Jong, A. Kuzmenko, M. Golden, and D. van der Marel, arXiv:0912.0636 (unpublished).
[12] B. Gorshunov, D. Wu, A. Voronkov, P. Kallina, K. Iida, S. Haindl, F. Kurth, L. Schultz, B. Holzapfel, and M. Dressel, Phys. Rev. B **81**, 060509(R) (2010).
[13] D. Wu, N. Barisic, P. Kallina, A. Faridian, B. Gorshunov, N. Drichko, L. Li, X. Lin, G. Cao, Z. Xu, N. Wang, and M. Dressel, Phys. Rev. B **81**, 100512(R) (2010).
[14] M. M. Qazilbash, J. J. Hamlin, R. E. Baumbach, M. B. Maple, and D. N. Basov, arXiv:0808.3748 (unpublished).
[15] Z. G. Chen, R. H. Yuan, T. Dong, and N. L. Wang, Phys. Rev. B **81**, 100502(R) (2010).
[16] G. F. Chen, Z. G. Chen, J. Dong, W. Z. Hu, G. Li, X. D. Zhang, P. Zheng, J. L. Luo and N. L. Wang, Phys. Rev. B **79**, 140509(R) (2009).
[17] R. Hu, E. S. Bozin, J. B. Warren and C. Petrovic, Phys. Rev. B **80**, 214514 (2009).
[18] L. Zhang, D. J. Singh, and M. H. Du, Phys. Rev. B **79**, 012506 (2009).
[19] C. C. Homes, M. A. Reedyk, D. A. Crandles, and T. Timusk, Appl. Opt. **32**, 2976 (1993).
[20] M. Dressel and G. Gruner, *Electrodynamics of Solids* (Cambridge University Press, Cambridge, 2001).
[21] L. Craco, M. Laad, and S. Leoni, arXiv:0910.3828 (unpublished).
[22] K. Haule, J. H. Shim, and G. Kotliar, Phys. Rev. Lett. **100**, 226402 (2008).
[23] G. D. Mahan, *Many-Particle Physics* (Plenum, New York, 1993).
[24] J. G. Proakis, *Digital Signal Processing*, 4th ed. (Prentice-Hall of India, New Delhi, 2007).
[25] U. Chatterjee, M. Shi, A. Kaminski, A. Kanigel, H. M. Fretwell, K. Terashima, T. Takahashi, S. Rosenkranz, Z. Z. Li, H. Raffy, A. Santander-Syro, K. Kadowaki, M. R. Norman, M. Randeria, and J. C. Campuzano, Phys. Rev. Lett. **96**, 107006 (2006).
[26] S. V. Dordevic *et al.* (unpublished).
[27] A. Subedi, L. Zhang, D. J. Singh, and M. H. Du, Phys. Rev. B **78**, 134514 (2008).
[28] Y. Xia, D. Qian, L. Wray, D. Hsieh, G. F. Chen, J. L. Luo, N. L. Wang, and M. Z. Hasan, Phys. Rev. Lett. **103**, 037002 (2009).
[29] S. V. Dordevic, L. W. Kohlman, L. C. Tung, Y.-J. Wang, A. Gozar, G. Logvenov, and I. Bozovic, Phys. Rev. B **79**, 134503 (2009).
[30] A. A. Schafgans *et al.* (unpublished).